Electrostatic Spin Crossover in a Molecular Junction of a Single-Molecule Magnet Fe_2

Hua Hao, XiaoHong Zheng, LingLing Song, RuiNing Wang, and Zhi Zeng*

Key Laboratory of Materials Physics, Institute of Solid State Physics, Chinese Academy of Sciences, Hefei 230031, People's Republic of China

(Received 18 July 2011; published 5 January 2012)

Spin crossover by means of an electric bias is investigated by spin-polarized density-functional theory calculations combined with the Keldysh nonequilibrium Green's technique in a molecular junction, where an individual single-molecule magnet $Fe_2(acpybutO)(O_2CMe)(NCS)_2$ is sandwiched between two infinite Au(100) nanoelectrodes. Our study demonstrates that the spin crossover, based on the Stark effect, is achieved in this molecular junction under an electric bias but not in the isolated molecule under external electric fields. The main reason is that the polarizability of the molecular junction has an opposite sign to that of the isolated molecule, and thus from the Stark effect the condition for the spin crossover in the molecular junction is contrary to that in the isolated molecule.

DOI: 10.1103/PhysRevLett.108.017202 PACS numbers: 75.50.Xx, 73.23.−b, 85.65.+h, 85.75.−d

Physical spin crossover (SCO) has attracted increasing attention because of its potential application in various domains, such as molecular spintronics [1–4], display devices, nonlinear optics, and photomagnetism [5]. Initial investigations showed that such a SCO could be achieved under external stimuli, such as a change of temperature, application of pressure, and light irradiation [6]. Nonetheless, for electronic applications it is more preferable to achieve a SCO purely by electric means. This would provide a useful platform for molecular spin-valve devices [7,8], magnetic molecule-based quantum computing [9], and other applications. On this topic, the spin-transfer torque mechanism [10] seems promising, but it is not easily accessible at the atomic scale owing to the large current densities required. Recently, Diefenbach and Kim [11] demonstrated a more practical SCO based on the Stark effect (or an electrostatic SCO), by concerning the distinct difference in response of molecular electronic states upon perturbation with an electric field. Baadji *et al.* [12] proposed an electrostatic magnetic-coupling transition (MCT, also a SCO) mechanism, by inspecting a model for superexchange in the presence of an external electric field. Moreover, they further calculated the critical field strength required for this MCT and proved that this strength could be attained by applying a moderate electric bias to a molecular junction.

In Refs. [11,12], two possible principles for the electrostatic SCO have been brought forward. Especially in Ref. [12], it is suggested that such a SCO observed in an isolated molecule will also appear in a realistic molecular junction so long as a large enough bias is applied. However, the SCO in an isolated molecule may disappear in a molecular junction even though the critical field strength for the SCO is attained by tuning the bias. The reason is that the environment is quite different in a molecular junction from an isolated molecule. In a molecular junction, the molecule-electrode coupling and the electron-density redistribution due to the electrodes can greatly influence the permanent dipole moment and response of electronic states upon the perturbation of an electric bias. Thus they can substantially affect the linear Stark effect, especially the polarizability and the quadratic Stark effect. Eventually, the SCO observed in an isolated molecule may be suppressed when it is set inside a molecular junction, and, moreover, the SCO which is absent in an isolated molecule could possibly exist in a molecular junction. Obviously, the effect of the electrodes on the Stark effect and the electrostatic SCO should be fully taken into consideration in a molecular junction, in order to make a more reliable prediction. This can be accomplished only by studying this problem more thoroughly in a realistic molecular junction.

In this Letter, we take a molecular junction, which consists of a single-molecule magnet $Fe_2(acpypentO) \times (NCO)_3$ [13] (abbreviated to SMM Fe_2) sandwiched between two Au(100) nanoelectrodes, as an example to investigate the electrostatic MCT (or SCO). The reason for choosing the SMM Fe_2 is that SMMs have great potential in molecular spintronics due to their appealing characteristics [2], and coordination compounds of iron(II) are common materials in which spin crossover occurs [6]. In order to more accurately explore the effects of the electrodes in a molecular junction, density-functional theory calculations are performed. Our results show that the electrostatic MCT appears in the molecular junction of the SMM Fe_2 but is absent in its isolated molecule. Then the mechanism for the MCT in a molecular junction is illustrated, and the reason for the substantial difference in the two situations is also analyzed.

Our theoretical calculations were performed with the program ATOMISTIX TOOLKIT [14], in which density-functional theory is combined with the Keldysh nonequilibrium Green's function method to calculate electronic and transport properties of nanoscale systems. The technical aspects of this method have been presented in great

details by Brandbyge *et al.* in Ref. [14]. The molecular junction we considered is that an individual SMM Fe_2 is connected by O1 and O2 atoms to two semi-infinite nanoscale Au(100) electrodes. Such nanoelectrodes are periodically arranged with 5, 4, 5, 4, ... atoms in the atomic layers along the z direction and has been adopted by many authors in the study of molecular devices [15–17]. The contact distance (d) between O and the surface of Au electrodes is chosen to be 1.8 Å. Four surface layers (5, 4, 5, and 4) of the left electrode and three surface layers (4, 5, and 4) of the right electrode in the central region are concerned to screen the perturbation effect of the SMM Fe_2 on the Kohn-Sham potential outside the central region, as shown in Fig. 1(b). A large enough vacuum layer (with a thickness of 20 Å) around the electrode in the x and y directions is chosen so that the device has no interactions with its mirror images. The exchange-correlation potential takes the form of the Perdew-Zunger parametrization of the local density approximation [18], because the local density approximation results regard the ferromagnetic state as the ground state of the isolated SMM Fe_2 molecule, which is consistent with the experiment [13]. Only valence electrons are self-consistently calculated, and the atomic cores are described by a standard norm-conserving pseudopotential [19]. The valence wave functions are expanded by localized numerical (pseudo)atomic orbitals [20], with the single zeta plus polarization basis set for Au atoms and the double zeta plus polarization basis set for other atoms.

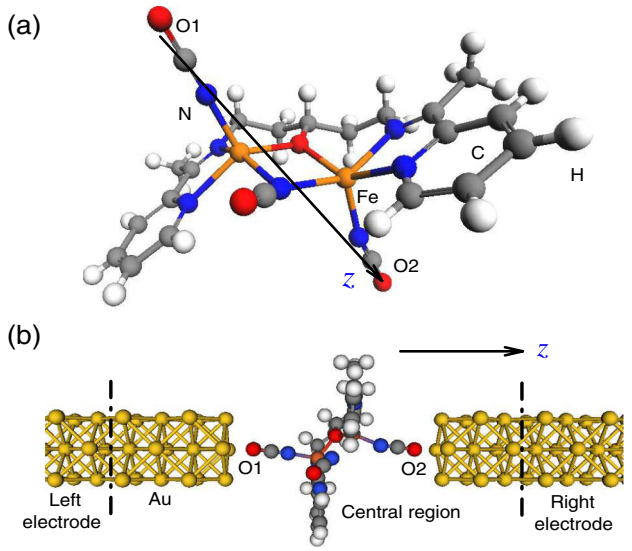

FIG. 1 (color online). (a) Geometrical structure of SMM Fe_2; (b) the model structure of the molecular junction: An individual SMM Fe_2 is sandwiched between two semi-infinite Au(100) electrodes. The part between the two dash-dotted lines is the central region, in which O1 and O2 atoms are used to be the contact atoms with the left (right) electrode. The contact distance between O1 (O2) and the surface of Au (100) is taken as $d = 1.8$ Å. The z direction in (a) is along the O1 and O2, the same as that in (b).

The Brillouin zone for the electrodes is sampled by a $1 \times 1 \times 100$ k-point grid. Before the calculations, the structural relaxation of the central molecule is carried out in this junction until the maximum ionic forces are smaller than 0.02 eV/Å.

A bias voltage (V_D) is applied along the z direction in a molecular junction by shifting the electrochemical potential of the left and the right electrodes $\mu_{l,r} = \mu(0)$ to $\mu_{l,r}(V_D) = \mu(0) \pm \mathrm{eV}_D/2$, where $\mu(0)$ is the average Fermi level of the system without bias. It is worth noting that in the calculation model V_D is also the voltage drop between the left side of the central region and the right side, which is regarded as a proper simulation of real experiments. The total energy of a molecular junction contains the free energy functional given by

$$E[n] = T[n] + E^{\mathrm{xc}}[n] + E^{H}[n] + E^{\mathrm{ext}}[n] - e\Delta N_L \mu_L - e\Delta N_R \mu_R. \quad (1)$$

The terms in the total energy equation are the kinetic energy of the Kohn-Sham orbitals $T[n]$; the exchange-correlation energy $E^{\mathrm{xc}}[n]$; the Hartree energy and the interaction energy with the pseudopotential ions $E^{H}[n]$; the interaction energy with an external field $E^{\mathrm{ext}}[n]$; and the electron density n of the central region. The last two terms describe the energy of the electrons which have entered the central region from either the left or the right reservoir ($-e\Delta N_L \mu_L$ and $-e\Delta N_R \mu_R$), arising from charge flow between the central region and the electron reservoirs. The number of electrons $\Delta N_{L,R}$ is calculated as the Mulliken charge of the atoms closest to the left (right) electrode, and $\mu_{L,R}$ is the electrochemical potential of the left (right) electrode. For simplicity, we denote the electrostatic energy of the molecular junction as $E_{\mathrm{ES}} = E^{\mathrm{ext}}[n] - e\Delta N_L \mu_L - e\Delta N_R \mu_R$.

In this molecular junction, the total energy in the FM state (ferromagnetic coupling of the two iron ions) is 59 meV lower than that in the AFM state (antiferromagnetic coupling of the two iron ions) when no electric biases are applied, as shown in Fig. 2(a). That means that the FM state is the ground state of the molecular junction, which is the same as the result of the isolated molecule [13]. In addition, the total energy of the molecular junction almost symmetrically rises as the bias increases from 0 to ± 0.6 V. More importantly, the total energy in the FM has some crossovers with that in the AFM under certain bias voltages [see the square region in Fig. 2(a)]. These crossovers indicate that the electrostatic MCT is realized in terms of the total energy. To clearly display the MCT, the magnetic-coupling constant as the function of the bias is defined as $J_{\mathrm{FM/AFM}} = [E_{\mathrm{FM}} - E_{\mathrm{AFM}}]/S^2_{\mathrm{max}}$, where $S_{\mathrm{max}} = 4$ is the maximum total spin of the SMM Fe_2. As shown in Fig. 2(b), a negative magnetic-coupling constant corresponds to the ferromagnetic coupling of the two Fe ions in the molecular junction, while a positive

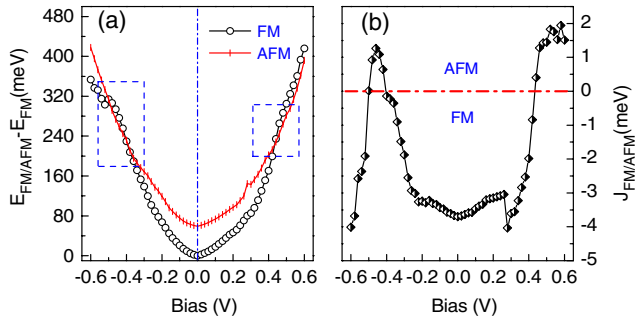

FIG. 2 (color online). (a) The total energy of the molecular junction under electric biases, relative to that of the ground state (the FM state) without electric biases. In the square, the total energy in the FM has some crossovers with that in the AFM. (b) The magnetic-coupling constant under electric biases.

magnetic-coupling constant corresponds to the antiferromagnetic coupling of them.

In order to understand the electrostatic MCT in this molecular junction, it is of first importance to comprehend the rise of the total energy with the increasing bias. Because of the symmetrical variation of the total energy under electric biases, a molecular junction with no permanent electric dipole will be a good model for this comprehension. In this model junction, the length of the central region is assumed to be L_{Tp}. When applying an electric bias (V_D), an uniform electric field (UEF) of $|\vec{E}_{\mathrm{UEF}}| = V_D/L_{\mathrm{Tp}}$ drives the electron-density redistribution, and then an inner field of $\vec{E}_{\mathrm{i}} \sim -\alpha\vec{E}_{\mathrm{UEF}}/\varepsilon$ is induced in the central region. The strength of the final field ($\vec{E}_{\mathrm{F}} = \vec{E}_{\mathrm{UEF}} + \vec{E}_{\mathrm{i}}$) is assumed to be smaller than that of the initial field in two regions ("L" and "R") and larger than that of the initial field in one region ("C") in this model junction, as shown in Fig. 3(a). Here, ε is a positive constant with the unit of eÅ^2/V, and the corresponding length is d_L, d_R, and d_C, respectively, for different regions. Given the above assumption, a positive polarizability ($\alpha_{L,R}^{\mathrm{Tp}} > 0$) is obtained in the region L and the region R, but a negative polarizability ($\alpha_C^{\mathrm{Tp}} < 0$) is obtained in the region C. From another viewpoint, an induced electric field is equivalent to an electric dipole moment $\vec{p}_{\mathrm{i}}$ ($= \alpha\vec{E}_{\mathrm{UEF}}$). This dipole moment interacts with the UEF, and then the electrostatic energy gain (EG) takes the form of the quadratic Stark energy: $\mathrm{EG}(\vec{E}) \sim -\alpha\vec{E}_{\mathrm{UEF}}^2$. Finally, the electrostatic energy gain of this model junction can be expressed as

$$\mathrm{EG}(\vec{E}) \sim -(\alpha_L^{\mathrm{Tp}} + \alpha_C^{\mathrm{Tp}} + \alpha_R^{\mathrm{Tp}})\vec{E}_{\mathrm{UEF}}^2. \tag{2}$$

Meanwhile, the equations

$$\begin{aligned}&(1 - \alpha_L^{\mathrm{Tp}})|\vec{E}_{\mathrm{UEF}}|d_L + (1 - \alpha_C^{\mathrm{Tp}})|\vec{E}_{\mathrm{UEF}}|d_C \\ &\quad + (1 - \alpha_R^{\mathrm{Tp}})|\vec{E}_{\mathrm{UEF}}|d_R \\ &= |\vec{E}_{\mathrm{UEF}}|(d_L + d_C + d_R) = |\mu_L - \mu_R|\end{aligned} \tag{3}$$

should be satisfied, in order to hold the potential drop during the electron-density redistribution. It is noteworthy that the potential profile in Fig. 3(a) is strongly dependent on the molecule-electrode coupling. Consequently, the overall polarizability of a molecular junction ($\alpha^{\mathrm{Tp}} = \alpha_L^{\mathrm{Tp}} + \alpha_C^{\mathrm{Tp}} + \alpha_R^{\mathrm{Tp}}$) calculated from Eqs. (2) and (3) can be greatly influenced by the molecule-electrode coupling. In particular, a negative polarizability ($\alpha^{\mathrm{Tp}} < 0$) can be obtained if $d_L, d_R > d_C$ is satisfied in a molecular junction, and thus the total energy will rise with the increasing bias.

To ensure the validity of the above model in the Fe_2 molecular junction, the polarizability is analyzed under the bias of 0.4 V. As shown in Fig. 3(b), a positive polarizability is indeed obtained in two regions, and a negative

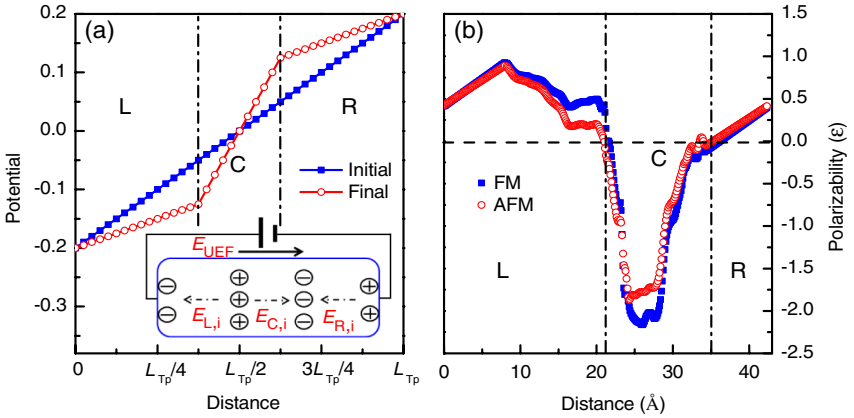

FIG. 3 (color online). (a) The schematic diagram of the potential profile in the central region of a molecular junction under electric biases. L_{Tp} is the length of the central region. L, R, and C denote regions where different electron redistribution occurs. The inset demonstrates the electron-density redistribution under an electric bias in the central region. $\vec{E}_{\mathrm{UEF}}$ is an uniform field generated by an electric bias, and $\vec{E}_{L(R,C),i}$ is the field induced by the electron-density redistribution. (b) The calculated polarizability for the FM and the AFM in the Fe_2 molecular junction under the bias of 0.4 V. In the regions L and R the polarizability takes a positive value, while in the region C the polarizability takes a negative value, which is the same as (a).

one in one region, which is qualitatively the same as the case in Fig. 3(a). Further analysis shows that α_L^{Tp} averagely equals to 0.62ε, α_C^{Tp} to -0.99ε, and α_R^{Tp} to 0.20ε in the FM, while in the AFM α_L^{Tp} averagely equals to 0.53ε, α_C^{Tp} to -0.86ε, and α_R^{Tp} to 0.20ε. Finally, the overall polarizability of the molecular junction (α^{Tp}) is -0.17ε in the FM and -0.13ε in the AFM. The above facts confirm the validity of the above model, depicted in Fig. 3(a). More importantly, we note that $|\alpha_{\mathrm{FM}}^{\mathrm{Tp}}|$ is larger than $|\alpha_{\mathrm{AF}}^{\mathrm{Tp}}|$, which is also true for other biases ranging from -0.5 to 0.6 V. The relation of $|\alpha_{\mathrm{FM}}^{\mathrm{Tp}}| > |\alpha_{\mathrm{AF}}^{\mathrm{Tp}}|$, together with $\alpha_{\mathrm{FM}}^{\mathrm{Tp}}, \alpha_{\mathrm{AF}}^{\mathrm{Tp}} < 0$, definitely leads to the crossovers of the total energy between the two magnetic states under a certain bias [see the square region in Fig. 2(a)].

For the isolated Fe_2 molecule, the total energy in the FM is 22 meV lower than that in the AFM when no electric fields are applied [21]. In addition, almost the same permanent electric dipoles ($\vec{p}$) are obtained in the two magnetic states. Based on the above fact and the electrostatic energy gain ($\mathrm{EG} \sim -\alpha^{\mathrm{Is}}\vec{E}^2 - \vec{p}\cdot\vec{E}$, $\alpha^{\mathrm{Is}} > 0$) used in Ref. [12], the MCT from FM to AFM in the isolated Fe_2 molecule is accessible only when $|\alpha_{\mathrm{FM}}^{\mathrm{Is}}| < |\alpha_{\mathrm{AF}}^{\mathrm{Is}}|$ is satisfied, as shown in Fig. 4(a). However, our calculations demonstrate that $|\alpha_{\mathrm{FM}}^{\mathrm{Is}}|$ is always larger than $|\alpha_{\mathrm{AF}}^{\mathrm{Is}}|$ in this molecule when an electric field is applied along the z direction. The actual relation of $|\alpha_{\mathrm{FM}}^{\mathrm{Is}}| > |\alpha_{\mathrm{AF}}^{\mathrm{Is}}|$ in the Fe_2 molecule is contrary to the relation of $|\alpha_{\mathrm{FM}}^{\mathrm{Is}}| < |\alpha_{\mathrm{AF}}^{\mathrm{Is}}|$ required for the MCT. As a result, the total energy in the FM has no such crossovers with that in the AFM, as displayed in Fig. 4(b).

From the above analysis of the electrostatic MCT in two different situations of the Fe_2 molecule (the isolated molecule and the molecular junction), we note that the relation of $|\alpha_{\mathrm{FM}}^{\mathrm{Tp(Is)}}| > |\alpha_{\mathrm{AF}}^{\mathrm{Tp(Is)}}|$ is in favor of the MCT only in the molecular junction, while in the isolated molecule the contrary condition ($|\alpha_{\mathrm{FM}}^{\mathrm{Is}}| < |\alpha_{\mathrm{AF}}^{\mathrm{Is}}|$) is required for the MCT. This difference between the two situations entirely arises from the relation of $\alpha^{\mathrm{Tp}} < 0 < \alpha^{\mathrm{Is}}$. The fundamental reason is that in a molecular junction the polarizability can be greatly changed by the molecule-electrode coupling, and, additionally, a fixed potential drop during the electron-density redistribution also has great impact on the polarizability. Thus from Eqs. (2) and (3), a negative polarizability is also possible in a molecular junction. Nevertheless, in an isolated molecule an electric field ($\vec{E}_{\mathrm{i}}$) is induced naturally in an opposite direction to the external electric field ($\vec{E}_{\mathrm{UEF}}$). As a result, the strength of the final field is always smaller than that of the initial field, schematically shown in Fig. 4(c). According to the relations of $\vec{E}_{\mathrm{F}} = \vec{E}_{\mathrm{UEF}} + \vec{E}_{\mathrm{i}}$ and $\vec{E}_{\mathrm{i}} \sim -\alpha\vec{E}_{\mathrm{UEF}}/\varepsilon$, a positive polarizability (α^{Is}) is always obtained for an isolated molecule.

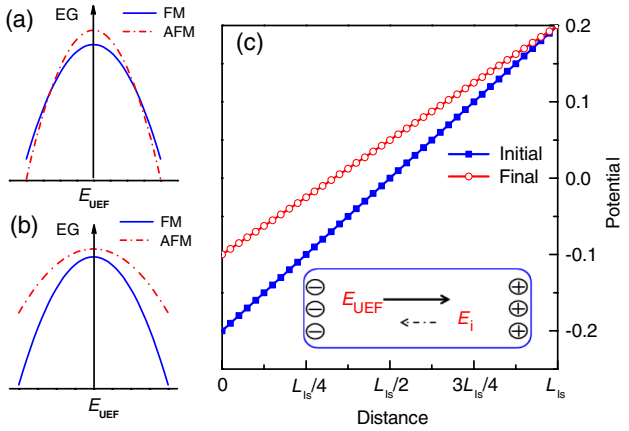

FIG. 4 (color online). The schematic diagram of the EG and the potential profile: (a) indicates the MCT from FM to AFM when $|\alpha_{\mathrm{FM}}| < |\alpha_{\mathrm{AF}}|$ is satisfied. (b) shows the actual electrostatic energy in the Fe_2 molecule under electric fields. (c) demonstrates the potential profile in an isolated system under an UEF, where L_{Is} is the length of this isolated system along the field direction, and the inset demonstrates the electron-density redistribution and the induced filed ($\vec{E}_{\mathrm{i}}$).

In the end, we would like to note that, in order to observe the electrostatic MCT in a realistic molecular junction, the central molecule, in which the polarizability is substantially different between two magnetic states (e.g., FM and AFM) under an electric field along the transport direction, is preferable. A good example is the phorphyrin nanoribbon molecular magnet [22], since the gap between the highest occupied and the lowest unoccupied molecular orbitals in the FM is greatly different from that in the AFM state, which suggests the substantial difference in the polarizability between the FM and the AFM states [11]. However, a molecule with the above feature is possibly, but not necessarily, favorable for the electrostatic MCT in a molecular junction, because the environment of a molecular junction can greatly affect the Stark effect and thus the electrostatic MCT.

In conclusion, we have investigated the electrostatic MCT (or SCO) in the Fe_2 molecular junction, in comparison with its isolated molecule. Our study demonstrates that the MCT from the FM state to the AFM state by electric fields exists only in the molecular junction but does not in its isolated molecule. The fundamental reason is that response of electronic states to an electric field is greatly affected by the molecule-electrode coupling in a molecular junction and also restricted by the potential drop. As a result, the relation of $\alpha^{\mathrm{Tp}} < 0 < \alpha^{\mathrm{Is}}$ is obtained in two different situations of the Fe_2 molecule, and, eventually, the condition for the MCT in this molecular junction is contrary to that in its isolated molecule.

This work was supported by the National Science Foundation of China under Grants No. 11104277, No. 11174289, and No. 10904148, National Basic Research Program of China (973) under Grant No. 2012CB93702, Director Grants of CASHIPS, and the Knowledge Innovation Program of Chinese Academy of

Sciences. The calculations were performed at Center for Computational Science of CASHIPS.

*Corresponding author.
zzeng@theory.issp.ac.cn

[1] S. Sanvito, J. Mater. Chem. **17**, 4455 (2007).
[2] L. Bogani and W. Wernsdorfer, Nature Mater. **7**, 179 (2008).
[3] M. Mannini, F. Pineider, P. Sainctavit, C. Danieli, E. Otero, C. Sciancalepore, A. M. Talarico, M.-A. Arrio, A. Cornia, D. Gatteschi, and R. Sessoli, Nature Mater. **8**, 194 (2009).
[4] W. Y. Kim, Y. C. Choi, S. K. Min, Y. Cho, and K. S. Kim, Chem. Soc. Rev. **38**, 2319 (2009).
[5] P. Gütlich and H. A. Goodwin, *Spin Crossover in Transition Metal Compounds I* (Springer-Verlag, Berlin, 2004).
[6] F. Renz, J. Phys. Conf. Ser. **217**, 012022 (2010).
[7] D. Waldron, P. Haney, B. Larade, A. MacDonald, and H. Guo, Phys. Rev. Lett. **96**, 166804 (2006).
[8] A. R. Rocha, V. M. García-suárez, S. W. Bailey, C. J. Lambert, J. Ferrer, and S. Sanvito, Nature Mater. **4**, 335 (2005).
[9] G. A. Timco, S. Carretta, F. Troiani, F. Tuna, R. J. Pritchard, C. A. Muryn, Eric J. L. McInnes, A. Ghirri, A. Candini, P. Santini, G. Amoretti, M. Affronte, and Richard E. P. Winpenny, Nature Nanotech. **4**, 173 (2009).
[10] Slonczewski, J. Magn. Magn. Mater. **159**, L1 (1996).
[11] M. Diefenbach and K. S. Tim, Angew. Chem., Int. Ed. **46**, 7640 (2007).
[12] N. Baadji, M. Piacenza, T. Tugsuz, F. D. Sala, G. Maruccio, and S. Sanvito, Nature Mater. **8**, 813 (2009).
[13] A. K. Boudalis, J. M. Clemente-Juan, F. Dahan, and J.-P. Tuchagues, Inorg. Chem. **43**, 1574 (2004).
[14] M. Brandbyge, J.-L. Mozos, P. Ordejón, J. Taylor, and K. Stokbro, Phys. Rev. B **65**, 165401 (2002); J. M. Soler, E. Artacho, J. D. Gale, A. Grcía, J. Junquera, P. Ordejón, and D. Sánchez-Portal, J. Phys. Condens. Matter **14**, 2745 (2002); J. Taylor, H. Guo, and J. Wang, Phys. Rev. B **63**, 245407 (2001).
[15] J. Taylor, H. Guo, and J. Wang, Phys. Rev. B **63**, 121104 (2001).
[16] B. Larade, J. Taylor, Q. R. Zheng, H. Mehrez, P. Pomorski, and H. Guo, Phys. Rev. B **64**, 195402 (2001).
[17] S.-H. Ke, H. U. Baranger, and W. Yang, Phys. Rev. B **71**, 113401 (2005).
[18] J. P. Perdew and A. Zunger, Phys. Rev. B **23**, 5048 (1981).
[19] N. Troullier and J. L. Martins, Phys. Rev. B **43**, 1993 (1991).
[20] E. Artacho, D. Sánchez-Portal, P. Ordejón, A. Grcía, and J. M. Soler, Phys. Status Solidi B **215**, 809 (1999).
[21] For the isolated SMM Fe_2, numerical calculations were performed by using spin-polarized density-functional theory with the Perdew-Burke-Ernzerhof exchange-correlation function [J. P. Perdew, K. Burke, and M. Ernzerhof, Phys. Rev. Lett. **77**, 3865 (1996)]; as implemented in the DMol^3 package [B. Delley, J. Chem. Phys. **92**, 508 (1990)].
[22] W. J. Cho, Y. Cho, S. K. Min, W. Y. Kim, and K. S. Kim, J. Am. Chem. Soc. **133**, 9364 (2011).